Enhancement of non-linear optical susceptibility in a superlattice with random constituent asymmetric multi-quantum wells

1998 J. Phys.: Condens. Matter 10 7691

(http://iopscience.iop.org/0953-8984/10/34/021)

J. Phys.: Condens. Matter **10** (1998) 7691–7700. Printed in the UK PII: S0953-8984(98)90226-0

Enhancement of non-linear optical susceptibility in a superlattice with random constituent asymmetric multi-quantum wells

Hang Dong† and Shi-Jie Xiong‡§

† The Fifth Department of High Power Radiation Laboratory under National 863 R.D. Program of Institute of Applied Physics and Computational Mathematics, Beijing 100088, People's Republic of China

‡ Chinese Centre of Advanced Science and Technology (World Laboratory), PO Box 8730, Beijing 100080, People's Republic of China

§ National Laboratory of Solid State Microstructure and Department of Physics, Nanjing University, Nanjing 210093, People's Republic of China

Received 29 December 1997, in final form 26 May 1998

Abstract. The optical third-order susceptibility of a superlattice consisting of randomly distributed asymmetric multi-quantum well units is theoretically studied. We carefully choose the randomness of thicknesses of the asymmetric multi-quantum well units to make sure that the spectrum has nearly equally separated energy minibands which give rise to the resonant enhancement of the third-order susceptibility owing to the multi-photon processes. Since the Bloch symmetry in the growth direction is partially violated due to the randomness, the inhibition of the transitions between states with different Bloch vectors is removed. Thus, the multi-photon processes are strengthened and the third-order susceptibility is greatly enhanced. The absorption coefficient of the random superlattice is also enhanced, but the photoabsorption is mainly a one-order process, its increase is far less than the third-order susceptibilities. Our calculation shows that, for the 150 layered superlattices, the ratio of third-order susceptibility to the absorption coefficient of a random superlattice can be about twenty times larger than that of the periodic superlattice.

1. Introduction

Band-gap engineering and molecular beam epitaxy make it possible to design man-made semiconductor structures with unusual electronic and optical properties. A large second-order susceptibility associated with a mid-infrared inter-level transition in asymmetric quantum wells has attracted wide attention in recent years [1–4]. At the same time, owing to the possible device applications, many groups have focused on the third-order non-linear susceptibility of semiconductors. It has been found that if the thicknesses of the layers in an asymmetric multi-quantum well are designed in such a way that the energy levels are nearly equally separated, the third-order susceptibility may be much enhanced owing to the resonant multi-photon processes. Calculations and observations of strong third-order non-linearity resonance have been reported in quantum wells and superlattices [5–9].

The calculation of the optical non-linearity for superlattices which consist of a large number of asymmetric multi-quantum well units shows that in some cases the coupling between the units may slightly enhance the magnitude of the third-order susceptibilities [6]. For the superlattices with translational symmetry in the growth direction, the conservation

0953-8984/98/347691+10$19.50

of momentum halts the inter-miniband transitions between the states with different Bloch vectors in this direction. It is predicted that if a superlattice is made of a random array of different types of asymmetric multi-quantum well units, the Block symmetry in the growth direction will be broken and the inhibition of inter-miniband transitions between states with different perpendicular momenta will be removed. This will greatly strengthen the multi-photon processes and, in turn, enhances the high-order susceptibility.

In the present paper we theoretically investigate the optical third-order susceptibility of a superlattice consisting of multi-quantum well units with random layer thicknesses. Every unit includes three wells and three barriers, which are alternately stacked. The unit layer thicknesses are designed in such a way that the lowest four levels of an isolated unit are nearly equally separated in energy. We slightly fluctuate the thickness of one barrier layer in each unit to form a random superlattice. Thus, the resultant minibands of the superlattice are still nearly equally separated in energy, but the translational symmetry in the growth direction is partially broken. We calculate the third-order susceptibility $\chi^{(3)}$ and compare the results with those obtained for the periodic superlattice with a similar unit structure. We find a remarkable enhancement of optical non-linearity due to the randomness. To clarify the absorption of light in such random structures we also calculate the absorption coefficient and find that the ratio of third-order susceptibility to the absorption coefficient of a typical random superlattice can be about twenty times larger than that of the periodic superlattice.

In the next section we will describe the structure of the random superlattice made of $GaAs/Al_xGa_{1-x}As$ multi-quantum wells. In section 3 we will calculate the third-order susceptibility and absorption coefficients for samples with different extents of randomness and different size, and discuss the conditions of enhancement of optical non-linearity. The results are summarized in section 4.

2. The structure of the random superlattice

It is known that an asymmetric multi-quantum well unit has a great $\chi^{(3)}$ if it has four nearly equally-spaced energy levels. To optimize $\chi^{(3)}$ we choose the structures of the basic unit in a superlattice so that for an isolated unit the lowest four energy levels are almost equally separated in energy. In an N-period superlattice the four levels are extended to four minibands, and every miniband has N states (not including spin).

We investigate the superlattice made of GaAs and $Al_xGa_{1-x}As$, corresponding to the well and barrier materials, respectively. The energy spectrum and wavefunctions of electrons are calculated by using the effective-mass approximation, taking into account the non-parabolicities in the dispersion relation of the layer materials:

$$\begin{aligned} E &= \frac{\hbar^2 q_1^2}{2m_1^*}(1-\gamma_1 q_1^2) + \frac{\hbar^2 k_\parallel^2}{2m_1^*} \qquad \text{for the wells} \\ E &= V - \frac{\hbar^2 q_2^2}{2m_2^*}(1-\gamma_2 q_2^2) + \frac{\hbar^2 k_\parallel^2}{2m_2^*} \qquad \text{for the barriers} \end{aligned} \tag{1}$$

where m_1^* and m_2^* are the effective masses of electrons in wells and barriers, respectively; γ_1 and γ_2 are the parameters describing the non-parabolicity of the bands, V is the height in energy of the barriers, q_1 and q_2 are the wavevectors in the growth direction in wells and barriers, respectively, and $k_\parallel$ is the parallel wavevector. To simplify the calculations we take $k_\parallel = 0$ without affecting the main results of the article.

The effective-mass parameters used here are taken from [10], that is, the barrier height is $V = f\Delta G$ with $f = 0.6$, and $\Delta G = 1.425x - 0.9x^2 + 1.1x^3$, the effective masses

are $m_1^* = 0.0665m_0$ and $m_2^* = (0.0665 + 0.0835\Delta G/1.625)m_0$ with m_0 being the mass of the free electron. The non-parabolicity coefficients for wells and barriers and the electron density in the wells are $\gamma_1 = 4.9 \times 10^{-19}$ m^2, $\gamma_2 = (m_1^*/m_2^*)^2\gamma_1$, $N_0 = 2 \times 10^{17}$ cm^{-3}, respectively [11]. The half linewidth at half maximum is taken from [12] with $\Gamma = 10$ meV for all the inter-miniband transitions. The doping density of Al in $Al_xGa_{1-x}As$ is set to be $x = 0.37$.

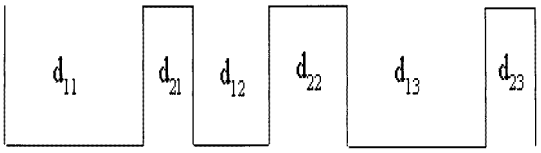

Figure 1. Structure of a multi-quantum well unit.

We use the multi-quantum-well as the basic unit for a superlattice, which includes three wells and three barriers, as illustrated in figure 1. From the parameters mentioned above we have determined its structure which satisfy the triply resonant condition, that is: $d_{11} = d_{13} = 2.9$ nm, $d_{12} = 6.5$ nm, $d_{21} = d_{23} = 1.6$ nm, $d_{22} = 4.0$ nm. We use this unit as a supercell to form a periodic superlattice. We construct two kinds of random superlattice by slightly fluctuating the thickness of the barrier in every unit with the following rule: (a) $d_{22} = 4.0[1 + (x_i - 0.5)\delta]$ nm, $d_{21} = d_{23} = 1.6$ nm; (b) $d_{22} = 4.0$ nm, $d_{21} = d_{23} = 1.6[1 + (x_i - 0.5)\delta]$ nm, where x_i is a random number uniformly distributed between 0 and 1, $i = 1, N$, δ is a constant representing the degree of randomness of the random superlattice.

We choose $\delta < 1.4$, corresponding to a small degree of randomness, to ensure the survival of the main features of the equal energy separation of the minibands. In figure 2, we show the energy band structures of the periodic and random superlattices by illustrating their densities of states. It is clear that the minibands of the random superlattice are slightly wider than that of the corresponding periodic one. With the increase of randomness of the superlattice, its energy band becomes wider and wider. The bandstructure ensures that the electrons in the random superlattice behave more like those in the periodic superlattice than in a free electron gas.

3. The third-order susceptibility of a random superlattice

To calculate the third-order susceptibility the following expression is used, which is a good approximation for the triply resonant case [11]

$$\chi_{3\omega}^{(3)} = \frac{e^4 N_0}{\varepsilon_0} \sum_{i,j,k,l=1}^{N} \frac{\langle z\rangle_{1i,2j}\langle z\rangle_{2j,3k}\langle z\rangle_{3k,4l}\langle z\rangle_{4l,1i}}{(\hbar\omega - \Delta E_{1i,2j} - \mathrm{i}\Gamma_{12})(2\hbar\omega - \Delta E_{1i,3k} - \mathrm{i}\Gamma_{13})(3\hbar\omega - \Delta E_{1i,4l} - \mathrm{i}\gamma_{14})} \tag{2}$$

where N_0 is the electron density in the wells, ε_0 is the permittivity of the vacuum, e is the electron charge, $\Delta E_{n\mu,m\nu}$ is the energy difference between the μth level of the nth miniband and the νth level of the ith miniband, and $\langle z\rangle_{n\mu,m\nu}$ is the dipole matrix element. We use the same transfer matrix method and the envelope function approximation as those adopted in [6] to calculate the matrix element of the inter-miniband transition, the non-parabolicities in the dispersion relation are taken into account.

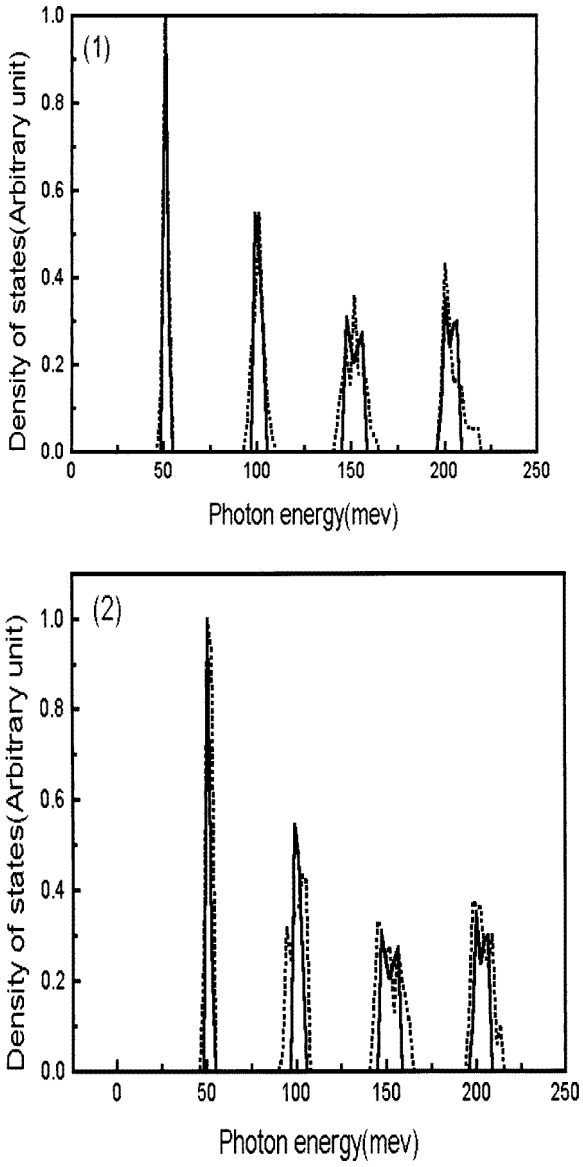

Figure 2. Density of states of periodic and random superlattices. The full curve is for a periodic superlattice and the dotted curve is for a random superlattice. $N = 150$. In figure 2(1) the random superlattice is constructed by method (a) and $\delta = 1.3$. In figure 2(2) the random superlattice is constructed by method (b) and $\delta = 0.6$.

The absorption character of the superlattice is also important in order to evaluate its nonlinear optical properties and its applicability. Apart from a constant factor, the absorption coefficient α of a superlattice can be written as [13]

$$\alpha(\bar{h}\omega) = (\bar{h}\omega)^{-1} \sum_{n,n'} |\hat{\varepsilon} \cdot P_{nn'}(0)|^2 \rho_{nn'}(\bar{h}\omega) \tag{3}$$

where $\rho_{nn'}(\omega)$ is the joint density of states associated with the nth and n'th energy minibands,

$P_{nn'}$ denotes the momentum matrix elements, $\hat{\varepsilon}$ is the unit vector in the direction of the light polarization. In this paper we choose $N_0 = 2\times10^{17}$ cm^{-3}. From (2) and (3) one can see that the virtual transitions are important for both the third-order susceptibility and the absorption coefficient. As we can see below, the randomness of the superlattice may create more possibilities for these transitions.

From figures 3 to 8 we present the calculated results of the third-order susceptibility and the absorption coefficient of random superlattices constructed by the above mentioned method (a) with different sizes and degrees of randomness. In figures 3 and 4 we plot $\chi^{(3)}$ and the absorption coefficient as functions of the photon energy for superlattices with different randomness of their layer thicknesses, with the total number of units being 150. The sample with $\delta = 0$ corresponds to a periodic superlattice. From the results we find that, with the extent of randomness δ increasing from 0 to 1.3, the absorption coefficient increases about five times, and the factor $\chi^{(3)}$ increases about one hundred times. $\chi^{(3)}$ increases much faster than the absorption coefficient.

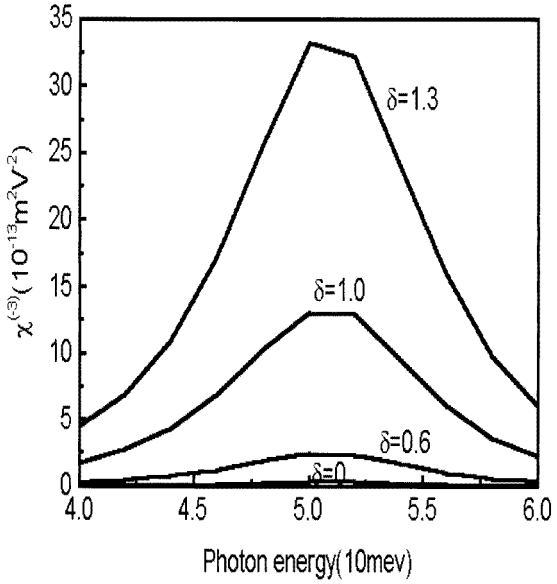

Figure 3. $\chi^{(3)}$ of superlattices with different randomness, $N = 150$.

In figure 5 we investigate smaller samples which consist of 40 units. In this situation we can see that when the degree of randomness is small, the $\chi^{(3)}$ of the sample is smaller than that of the periodic ones, showing a different behaviour from that of figure 3 in which the sample is larger. This is because of the competition of two opposite effects of the randomness: on the one hand the randomness of layer thicknesses breaks the translational symmetry, releases the inhibition for the transition between states with different perpendicular momentum and, in turn, strengthens the non-linearity resonance. On the other hand, it shifts the minibands and partially violates the resonance in the multi-photon processes. When both the number of layers and the degree of randomness are small, the former effect is weaker and the latter effect becomes dominant. With the increase of the layer number or the degree of randomness, the former effect becomes important, and the $\chi^{(3)}$ of the random superlattice begins to increase and eventually becomes much larger than that of the periodic ones. The shift of the resonant frequency for one unit of a random

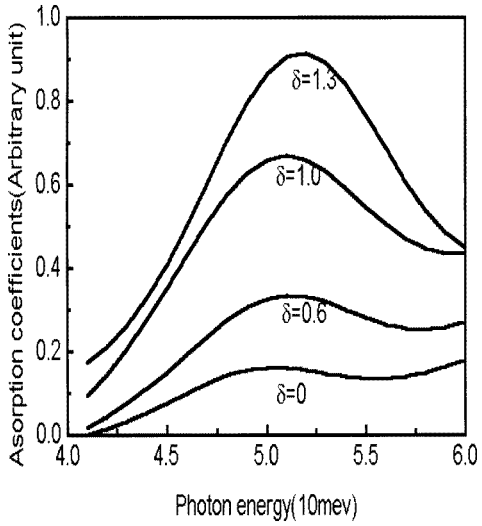

Figure 4. Absorption coefficients of superlattices with different randomness, $N = 150$.

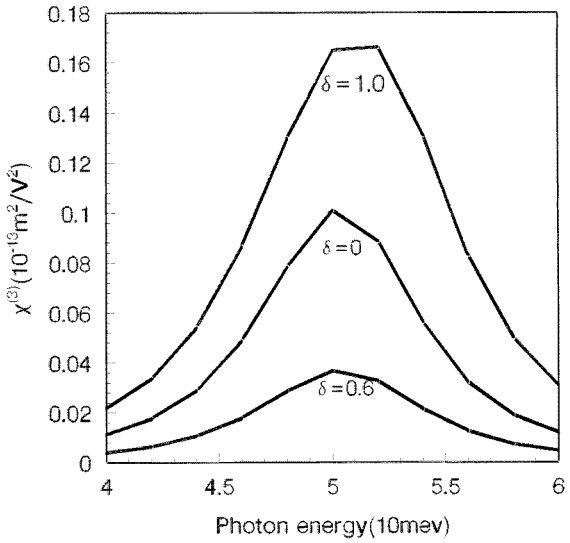

Figure 5. $\chi^{(3)}$ of the superlattice with different randomness, $N = 40$.

sample depends on its specific structure and fluctuates from unit to unit. The frequency dependence of the peak $\chi^{(3)}$ reflects the average of the unit resonant frequencies and is almost unchanged by changing the degree of randomness, as can be seen from the figures.

In figures 6, 7 and 8 we plot the ratio of the third-order susceptibility to the absorption coefficient. In figure 6 we illustrate the ratio of $\chi^{(3)}$ to the absorption coefficient for samples with different degrees of randomness. It shows that the ratio of the sample with $\delta = 1.3$ is about 20 times larger than that of the sample with $\delta = 0$. In figures 7 and 8 we plot the ratio of $\chi^{(3)}$ to the absorption coefficient of the samples with a different number of layers. We find that, with the number of layers increasing from 40 to 150, for the random superlattice

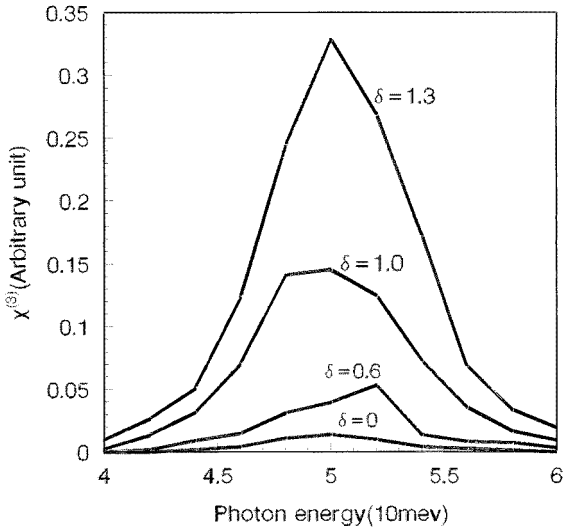

Figure 6. The ratio of $\chi^{(3)}$ to the absorption coefficient of the superlattice with different randomness, $N = 150$.

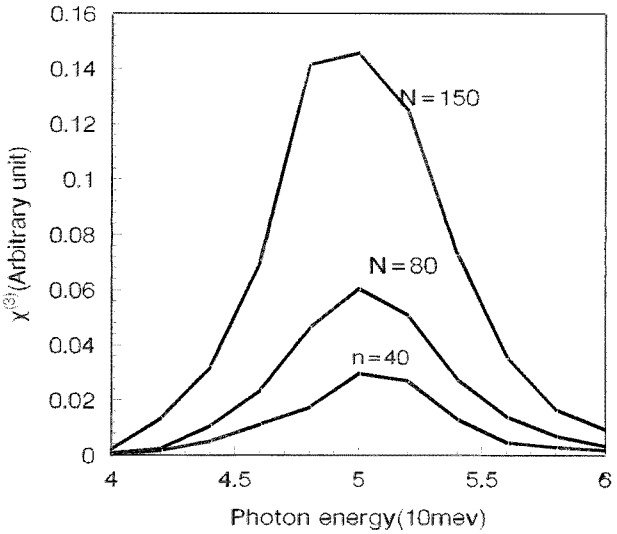

Figure 7. The ratio of $\chi^{(3)}$ to the absorption coefficient of the superlattice with different numbers of layers, $\delta = 1.0$.

the ratio increases and for the periodic ones the ratio decreases. This means that the random superlattice has better non-linear optical properties and applicability.

In figure 9 we show the $\chi^{(3)}$ of samples constructed by different methods. Because the sample constructed by method (b) has a random thickness distribution in two barriers of each unit, it is more random than that constructed by method (a) with the same δ, and the $\chi^{(3)}$ of such a sample is larger. This fact strengthens the effect that greater randomness induces larger $\chi^{(3)}$.

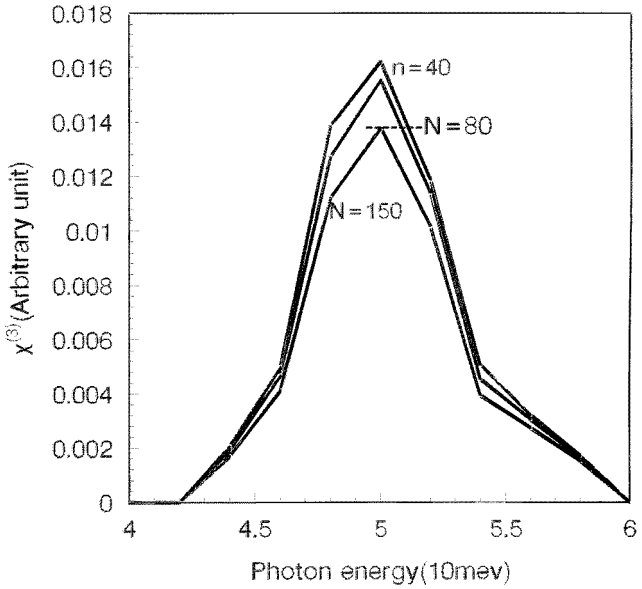

Figure 8. The ratio of $\chi^{(3)}$ to the absorption coefficient of the superlattice with different numbers of layers, $\delta = 0.0$.

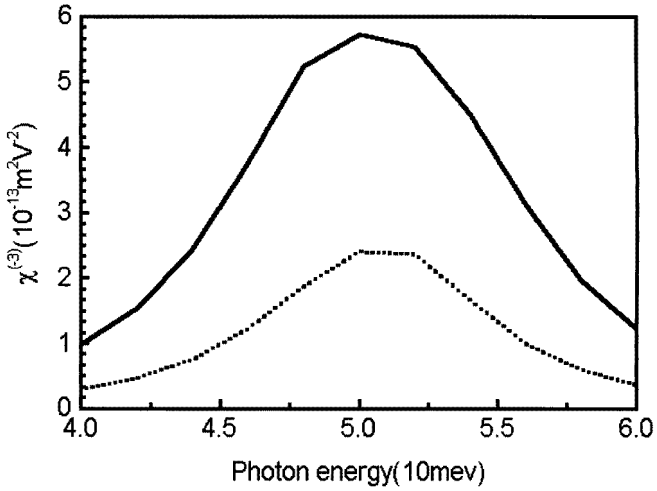

Figure 9. $\chi^{(3)}$ of superlattices with different randomness, $N = 150$, $\delta = 0.6$. The broken curve is for the sample constructed by method (a), and the full curve is for the sample constructed by method (b).

In figure 10 we show the ratio of the real to imaginary part of $\chi^{(3)}$ of the periodic and random superlattice. We find that the dependence of this ratio on the frequency is almost the same for the random and periodic samples. This means that the randomness has no effect on this quantity because in both cases the basic mechanism for the resonant $\chi^{(3)}$ is the same.

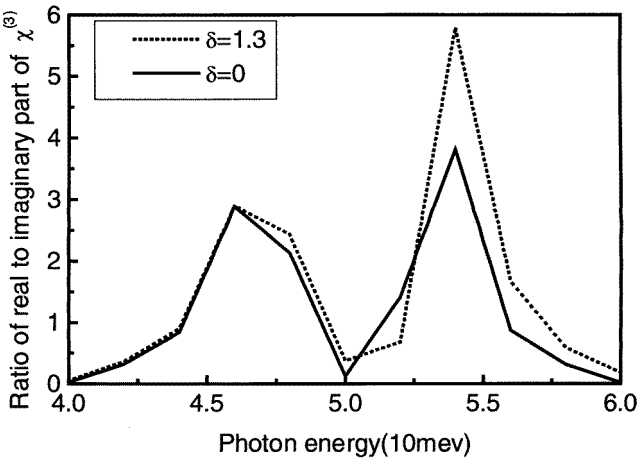

Figure 10. Ratio of the real to imaginary part of $\chi^{(3)}$, $N = 150$. The random sample is constructed by method (a).

4. Conclusions

In summary, we have analysed the third-order susceptibility and absorption coefficient of superlattices consisting of asymmetric multi-quantum well units with random layer thicknesses and compared the results with those of the corresponding periodic samples. The randomness of the structure produces two effects on the value of the third-order susceptibility: (1) it shifts the subbands and partially violates the resonance in the multi-photon processes; (2) it breaks the translational symmetry in the growth direction and removes the transition inhibition for the initial and final states with different perpendicular wavevectors. Our results show that for a small sample and small degree of randomness the former is more important and the resultant non-linear optical susceptibility is reduced by the randomness. In the system with large enough unit number, however, the latter becomes dominant and the $\chi^{(3)}$ is remarkably enhanced. The absorption coefficient of the random superlattice is also enhanced but, only one-order of magnitude, this increase is much smaller than the increase of $\chi^{(3)}$. Our results show that the $\chi^{(3)}$ of the random superlattice can be about 100 times larger than that of the corresponding periodic superlattice, and the ratio of $\chi^{(3)}$ to the absorption coefficient can be 20 times larger. Nevertheless, the random structure provides a possible approach with which to improve the optical non-linearity of the materials.

Acknowledgments

This work was supported by the National Foundation of Natural Science and the Youth Science Fund of Laser Technology of China.

References

[1] Rosencher E, Bois P, Nagle J, Costard E and Delaitre S 1990 *Appl. Phys. Lett.* **56** 1822
[2] Sirtori C, Capasso F, Sivco D L, Cu S N G and Cho A Y 1991 *Appl. Phys. Lett.* **59** 230
[3] Walrod D, Auyang S Y, Wolf P A and Sugimoto M 1991 *Appl. Phys. Lett.* **59** 2932
[4] Chenhsin Lien, Yimin Huang and Tan-FuL Lei 1994 *J. Appl. Phys.* **75** 2177

[5] Sirtori C, Capasso F, Sivco D L and Cho A Y 1992 *Phys. Rev. Lett.* **68** 1010
[6] Hang Dong and Shi-Jie Xiong 1994 *J. Appl. Phys.* **76** 2455
[7] Grave L, Segev M and Yariv A 1992 *Appl. Phys. Lett.* **60** 2717
[8] Yimin Huang 1994 *J. Appl. Phys.* **75** 3223
[9] Khurgin J B and Li S 1993 *Appl. Phys. Lett.* **62** 126
[10] Shen Y R 1984 *The Principles of Nonlinear Optics* (New York: Wiley)
[11] Nelson D F, Miller R C and Leinman D A 1987 *Phys. Rev.* B **35** 7770
[12] Krahl M, Christen J and Bimberg D 1987 *Gallium Arsenide and Related Compounds 1987: Proc. 14th Int. Symp. Gallium Arsenide and Related Compounds (Heraklion, Crete)* ed Christou and H S Rupprecht p 411
[13] Chen Xiao Shuang and Xiong Shi-Jie 1993 *Phys. Rev.* B **47** 7146